JOURNAL OF SUSTAINABLE MATERIALS PROCESSING AND MANAGEMENT
e-ISSN: 2821-2843

JSMPM

Vol. 5 No. 2 (2025) 104-121
https://publisher.uthm.edu.my/ojs/index.php/jsmpm

Optimization of Fatigue Strength in Sand-Cast Aluminium Alloys Using Waste Metal Chips as Mold Additives

Maaruf Isyaku[1]*, Danjuma Saleh Yawas[1,2], Mathew Olatunde Afolayan[1], Terva Ause[3], Tanimu Kogi Ibrahim[4]

[1] *Mechanical Engineering Department, Ahmadu Bello University, Zaria, NIGERIA*
[2] *Shell JV Professorial Chair Office, Mechanical Engineering Department, Ahmadu Bello University, Zaria, NIGERIA*
[3] *Metallurgical and Materials Engineering Department, Ahmadu Bello University, Zaria, NIGERIA*
[4] *Mechanical Engineering Department, Federal University Wukari, Wukari, Taraba State, NIGERIA*

*Corresponding Author: terrytanimu@yahoo.com
DOI: https://doi.org/10.30880/jsmpm.2025.05.02.009

Article Info

Received: 1 August 2025
Accepted: 18 November 2025
Available online: 10 December 2025

Keywords

Alumunium alloy casting, metal chips, grain refinement, fatigue strength, sand mould optimization

Abstract

This study investigates the enhancement of fatigue strength in aluminium alloy castings obtained from scrap engine blocks, through grain refinement achieved by incorporating metal chips into sand molds during sand casting. The materials used included a scrap engine block (aluminum alloy), molding sand, and chips from cast iron and brass, all of which were procured and characterized. Using a Taguchi design of experiment, alloys were cast with varying proportions of particle sizes and amounts of brass and cast iron chips. XRF analysis identified aluminium (76.61%), silicon (17.49%), and magnesium (1.28%) as the primary elements in the scrap aluminium alloy, while brown sand predominantly contained silicon (89.51%) and phosphorus (7.41%). The cast iron was mainly composed of iron (88.3%), carbon (3.7%), and silicon (2.3%). Fatigue testing results indicated a 24.78% increase in strength compared to the as-cast alloy, with Taguchi optimization yielding a further improvement of 28.30%. The optimal configuration found included brass/cast iron metal chips at level 2, a chip content of 40 %wt (level 4), and a chip particle size of 100 µm (level 1), resulting in a fatigue strength of 70.58 MPa. SEM and optical micrographs of the optimal sample showcased a finer grain structure. Thermogravimetric analysis revealed a 3.01% reduction in mass loss and a 33.11% increase in decomposition onset temperature compared to the control, indicating enhanced thermal stability. Furthermore, using foundry sand mixed with metal chips yielded improvements in green compressive strength of 20.33%, dry compressive strength of 22.73%, and compactability of 4.55%. Overall, this study confirms that integrating metal chips into sand molds significantly enhances both the fatigue strength of aluminium alloy castings and the quality of the molds, presenting promising implications for the recycling and utilization of scrap materials in casting processes.

1. Introduction

Long-term durability of structural and functional components, especially those subjected to cyclic or fluctuating loads, is strongly governed by their fatigue strength. Fatigue failure accounts for a significant percentage of in-service mechanical failures, particularly in automotive, aerospace, marine, and manufacturing industries [1]. Unlike static failures, fatigue cracks initiate and propagate over time under repeated or reversed stress cycles, often below the material's ultimate tensile strength. Thus, enhancing fatigue strength is paramount for ensuring the reliability and safety of engineering components such as engine connecting rods, crankshafts, brake discs, gears, and turbine blades [2-5].

In the context of metal casting, particularly aluminium alloy castings manufactured via sand casting, achieving a microstructure conducive to high fatigue resistance remains a critical challenge. Sand, the traditional mold material in most foundries, is inherently a poor conductor of heat. This poor thermal conductivity slows down the rate of heat extraction during solidification, leading to the development of coarse grains within the cast structure. Coarse-grained microstructures are prone to early crack initiation and rapid fatigue crack propagation due to the presence of larger slip planes and more significant stress concentration zones [6-10].

Grain refinement during solidification is widely recognized as one of the most effective means of improving fatigue strength. Fine-grained metals exhibit higher resistance to fatigue crack initiation because of their refined microstructure and increased grain boundary area, which acts as a barrier to dislocation movement. Traditionally, methods such as melt superheating, chemical grain refiners, electromagnetic stirring, or mechanical agitation have been employed to achieve fine grains. However, these methods are often costly, energy-intensive, and environmentally burdensome. There is a growing need for sustainable, low-cost, and effective grain refinement techniques that can be easily adopted in conventional sand-casting foundries, especially in resource-constrained settings [11-13].

The present research proposes an innovative approach to grain refinement by modifying the mold composition in sand casting using a mixture of metal chips, specifically brass and cast iron, combined with traditional foundry sand. This mixture enhances the thermal conductivity of the molding media, thereby promoting rapid solidification and fine-grain formation in the cast aluminium alloy. By doing so, the resulting components are expected to exhibit significantly improved fatigue strength. This novel method not only enhances performance but also aligns with the global agenda for sustainable manufacturing, particularly the United Nations Sustainable Development Goals (SDGs): SDG 9 (Industry, Innovation, and Infrastructure), SDG 12 (Responsible Consumption and Production), and SDG 13 (Climate Action) [14].

Reusing metal chips, a by-product of machining processes, serves a dual function in this research. First, their high thermal conductivity contributes to increased solidification rates and finer microstructures. Second, their incorporation into molding sand offers a responsible and eco-friendly method of waste management. If not properly handled, metal chips pose serious environmental threats, especially when dumped indiscriminately in water bodies, roadsides, or agricultural lands. Their utilization in casting processes transforms waste into a resource, reducing environmental hazards and encouraging circular economy principles in line with SDG 12 [15-17].

Furthermore, the traditional limitations of sand casting in terms of slow heat extraction and, by extension, poor fatigue properties, are directly addressed in this study. In many developing countries, over 1,000 foundries collectively produce approximately 1.5 million tons of castings annually. According to various industrial reports, sand casting remains the dominant method used due to its simplicity, low cost, and suitability for a wide range of applications [18]. These foundries supply critical agricultural, construction, and transportation components. Improving the fatigue life of these components using a low-cost, environmentally friendly, and scalable solution can significantly enhance the reliability and competitiveness of local manufacturing [19].

The fatigue behaviour of aluminium alloys is sensitive to both macro and microstructural features. Surface finish, casting porosity, grain size, and inclusions or intermetallic phases all influence fatigue crack initiation and propagation. Coarse grains serve as easy pathways for crack growth due to reduced grain boundary hindrance, whereas fine grains distribute the stress more evenly and delay crack nucleation [20]. Therefore, ensuring a fine and uniform grain structure is key to improving the fatigue strength of cast components [20-21].

This study uses various proportions of brass and cast iron chips mixed with foundry-grade silica sand to form modified molding mixtures. The heat transfer characteristics of these mixtures are expected to improve significantly over pure sand, enabling faster heat extraction from the molten metal during casting. This will lead to reduced dendritic arm spacing, minimized porosity, and refined grain structure all of which contribute positively to fatigue resistance. The study uses the Taguchi experimental design to systematically vary the chip proportions, particle sizes, and types, followed by fatigue testing and microstructural characterization to determine the optimal conditions for maximizing fatigue strength.

The results of this investigation are not only expected to improve component performance but also demonstrate a model of sustainable engineering practice. The process reduces the carbon footprint of casting operations by using waste metal chips as functional material enhancers. It aligns with SDG 13 by contributing to

climate mitigation through waste reduction and process efficiency. Moreover, since the method does not require specialized equipment or complex technology, small-scale foundries can readily adopt it, fostering inclusive and sustainable industrial growth (SDG 9).

The broader significance of enhancing fatigue strength through sustainable grain refinement also lies in the lifecycle extension of components. Longer-lasting parts reduce the need for frequent replacements, which lowers raw material demand, production energy, and transportation emissions, contributing to a cleaner, more efficient production ecosystem. Additionally, this reduces costs for end-users and industries, making the solution environmentally viable and economically beneficial.

2. Materials and Methods

2.1 Materials

The materials used in this study included aluminium-silicon alloy scrap (sourced from a discarded engine block at Pantaka Market, Kaduna), foundry sand, bentonite, machined grey cast iron chips, brass chips, grinding papers, polishing cloth and powder, cotton wool, and etchant. The equipment used comprised a vibrating sieve shaker, permeability meter, standard sand rammer, XRF machine, universal sand strength testing machine, digital weighing balance, charcoal-fired crucible furnace, optical microscope, polishing machine, CNC lathe machine, and a fatigue testing machine.

2.2 Experimental Procedure

2.2.1 Collection of Samples

Cast iron chips were sourced from an automobile workshop in Tudun Wada, Zaria, Nigeria. These chips were obtained from the re-boring of engine blocks of 10-seater Toyota buses, which were made of cast iron. Brass chips were collected from a machining shop at Panteka Market, Kaduna, Nigeria. The foundry sand used in the study was obtained from the Zaria Dam within Ahmadu Bello University, Zaria, Nigeria.

2.2.2 Sieving of the Collected Metal Chips and Molding Sand

The sand and metal chips were sieved using a vibrating sieve shaker in the foundry workshop of the Department of Metallurgical and Materials Engineering, Ahmadu Bello University, Zaria. The sand grain size was determined by calculating the Grain Fineness Number (GFN), which reflects the average particle size and is based on the American Foundry Society (AFS) standard. A standard set of sieves was used, which were arranged from coarsest at the top to finest at the bottom. A 100 g sample of sand was placed on the top sieve and subjected to vibration for 20 minutes. After sieving, the retained sand on each sieve was weighed. Each weight was multiplied by the corresponding sieve mesh number, and the sum of these products was divided by the total sample weight to calculate the GFN [22]. The sieve analysis results are presented in Table 1.

Table 1 *The result of the sieve analysis of the silica sand*

S/N	Mesh Size (mm)	Weight Retained
1	1.40	-
2	1.00	-
3	0.71	0.40
4	0.50	12.33
5	0.35	43.30
6	0.25	31.12
7	0.18	6.27
8	0.13	3.38
9	0.09	1.09
10	0.06	1.05
11	PAN	0.91
12	Total	99.85

*Notes: total weight of sample = 100g; time of shaking = 15mins

2.2.3 Planning Experiment Runs

The experimental runs were planned using the Taguchi design approach, which was implemented with Minitab Statistical Software. This study investigated three factors: type of chips, chips content, and chips particle size, each at four levels. Table 2 details these factors and levels used to produce a standard Taguchi L_{16} (4x3) orthogonal array design, presented in Table 3. The chip types were defined as: 1 = cast iron chips, 2 = brass chips and cast iron chips (1:2 ratio), 3 = brass chips and cast iron chips (2:1 ratio), and 4 = brass chips.

Table 2 *Sand mold parameters and their levels for the production of aluminium alloy*

S/N	Processing Factors	Factors Designation	Level			
			1	2	3	4
1	Chips Type	A	1	2	3	4
2	Chips Content (%)	B	10	20	30	40
3	Chips Particle Size (µm)	C	100	200	300	400

Table 3 *L_{16} orthogonal array of sand mold composition for aluminium alloy production*

Runs	Factors		
	A	B (wt%)	C (µm)
1	1	1	1
2	1	2	2
3	1	3	3
4	1	4	4
5	2	1	2
6	2	2	1
7	2	3	4
8	2	4	3
9	3	1	3
10	3	2	4
11	3	3	1
12	3	4	2
13	4	1	4
14	4	2	3
15	4	3	2
16	4	4	1

2.2.4 Mixing of Various Blends

The different molding sand blends were prepared by mixing sand with varying proportions and particle sizes of metal chips, as specified in each experimental run in Table 3. The sand and metal chips were weighed using a digital scale and poured onto a metallic table. A sand binder consisting of 2% bentonite was added, followed by 5% water. The mixture was then thoroughly blended using an electromechanical mixing machine for 5 minutes to minimize water loss through evaporation. A control sample was also prepared using only sand, 2% bentonite, and 5% water without metal chips. This control mixture served as a reference for comparison with the metal chip-reinforced blends during casting.

2.2.5 Molding Procedure for Production of Aluminium Alloy

A cylindrical pattern measuring 15 mm in diameter and 300 mm in length was fabricated from a stainless steel pipe to ensure the cast product had sufficient size for mechanical testing. The molding box was first positioned, and a small amount of molding sand was poured in and rammed to a height of 20 mm from the base. The cylindrical pattern was then placed on the compacted base. Additional molding mixture was added to fill the box, followed

by further ramming to achieve proper compaction. Excess sand was trimmed off after final ramming. The pattern was then carefully withdrawn vertically to form the desired cavity in the mold.

2.2.6 Melting and Casting

The aluminium alloy used for melting was sourced from a discarded automobile engine block, which was broken into smaller pieces to facilitate charging into a charcoal-fired crucible furnace. A medium-sized crucible was selected based on the total volume of the mold cavities. The furnace was fired and preheated for about 30 minutes before adding the aluminium alloy. Melting continued with increased firing until a temperature of 804 °C above the alloy's melting point was reached, ensuring sufficient fluidity, as recommended by Kang et al. [23]. The firing was then reduced, allowing the temperature to drop to around 720 °C, at which point the molten metal was poured into the mold cavities. A type-X thermometer, ranging from -50 °C to 1350 °C, was used to monitor the temperature. After pouring, the castings were left to solidify and cool to room temperature before shakeout. The cast bars were removed, collected, and labelled according to their respective sand-metal chip blend compositions. The Processes from ramming to casting are shown in Fig. 1.

Fig. 1 *Casting processes of the aluminium alloy; (a) Mechanical sand mixer; (b) Ramming process; (c) Prepared mold for casting; (d) Pouring of molten metal; (e) Cast aluminum alloys*

2.2.7 Production of Standard Test Samples from the Optimally Formulated Molding Sand for Foundry Properties Evaluation

Based on the formulation, cylindrical test samples with standard dimensions of 5 cm in height and 5 cm in diameter were produced after the ramming operation. Each sample was compacted by applying three blows using the ramming machine shown in Fig. 2(a). Fig. 2(b) displays the resulting cylindrical molded test sample.

(a) Green Compression Strength Test

A standard universal sand strength testing machine was used, as shown in Fig. 2(c). The prepared samples were mounted using a compression-holding device. The test was conducted by applying a uniformly increasing load of 5 kN, achieved by rotating the machine's lever clockwise until the specimen failed. The reading on the scale at the point of failure was recorded as the compressive strength.

(b) Dry Compression Strength Test

The standard green test samples were placed in an oven and baked at 110 °C for one hour. After baking, the samples were removed, allowed to cool, and tested using the same procedure described for the green compression test. The compressive strength values were recorded accordingly.

(c) Compactibility Test

The prepared specimen, contained within a standard tube, was placed in the rammer machine. It received five consecutive blows from the 6.35 kg rammer head. The compactibility was determined by measuring the movement between the fourth and fifth blows, referencing a scale where zero travel indicates maximum compactibility. This test was performed on all formulated molding sand mixtures.

(a) **(b)** **(c)**

Fig. 2 *Standard sand rammer*

2.3 Mechanical and Microstructural Properties Tests

2.3.1 Machining of the Cast Bars into Standard Test Samples

The cast cylindrical aluminium alloy bars were cut and machined on a CNC machine in the Mechanical Engineering Department workshop at Ahmadu Bello University, Zaria. These bars were prepared into standard samples for both fatigue and microstructural analyses.

2.3.2 Fatigue Test

The fatigue test was conducted at the Mechanical Engineering Department workshop, Ahmadu Bello University, Zaria, Nigeria using AVERY 7304 fatigue testing machine. The rods were cut and machine according to ASTM D31-99. The specimens shown in Fig. 3(a) were subjected to cyclic loading at constant stress amplitudes, typically below the material's yield strength [45]. Testing continued until the specimens failed, as Fig. 3(b) shows the failed samples.

(a) **(b)**

Fig. 3 *Samples for fatigue test*

2.3.3 Metallographic (Microstructural) Examination

Microstructural analysis was performed using an optical microscope in the Department of Metallurgical and Materials Engineering, Ahmadu Bello University, Zaria. Polishing was done using a METASERV universal polishing machine with two 15 cm diameter rotating discs, fitted with synthetic velvet cloths and 1 µm alumina paste. The samples were etched for 10 seconds using a solution of 5 ml nitric acid, 2 ml hydrofluoric acid, and 100 ml distilled water. After etching, the samples were examined under a digital optical metallurgical microscope at 100× magnification, and images were captured. Subsequently, the samples were analyzed using a scanning electron microscope (SEM) to observe and document their surface microstructures [24-26].

2.3.4 Optimization, Regression Analysis and Grey Relational Analysis

The experimental properties of the developed aluminum alloy were analyzed using the Taguchi optimization method and regression analysis with the aid of Minitab and Origin 2020 (OriginLab) software, respectively.

2.4 Taguchi Optimization

A standard method for evaluating the strength of relationships between sequences is the signal-to-noise (S/N) ratio, as defined by the Taguchi method. According to Taguchi, the S/N ratio falls into three categories: nominal-the-better, higher-the-better, and lower-the-better (Montgomery, 2001). In this study, the higher-the-better criterion was applied to analyze the properties of the aluminium alloy, using the S/N ratio (η) function shown in Equation 1 [27-30]:

$$\eta = -10\log_{10}\left(\frac{1}{n}\sum_{i=1}^{n}\frac{1}{y_i^2}\right) \quad (1)$$

Where n is the sample size and y_i is the response of the run.

2.4.1 Estimating the Optimal Values

The predicted optimum value of the means or S/N ratio (T_{opt}) of the response was determined by Equation 2 [31-34].

$$T_{opt} = T_m + \sum_{k=1}^{k_n}\left[\left(T_{ij}\right)_{max} - T_m\right] \quad (2)$$

Where: T_m is the overall mean or S/N ratio; $(T_{ij})_{max}$ is the mean or S/N ratio of the optimum level (i) of factor k and k_n is the number of main design factors that affect the response. T_{ijmax} is obtained from the main effect graph of mean or S/N ratio for each parameter; the highest value among the levels is the $(T_{ij})_{max}$.

2.4.2 Confirmation Experiment

A confirmation experiment was conducted using the optimum settings to verify the predicted fatigue strength under those conditions. A new aluminium alloy sample was cast using the identified optimum factor levels to validate the Taguchi-optimised parameters. The confirmation test was then conducted according to ASTM standards, with three replications performed to ensure accuracy and reliability [34, 35].

2.4.3 Confidence Interval (CI)

For this study, the experimental value is expected to fall within this range below;

$$\text{Predictive} - \text{CI} < \text{Experimental} < \text{Predictive} + \text{CI} \quad (3)$$

Where predictive is the predicted or optimum Fatigue strength, experimental is the experimental value after the confirmation test, while CI is the Confidence Interval. Equation 4 was used to evaluate the CI [35].

$$C.I. = \sqrt{f_{\propto(1,d_e)} v_e \left(\frac{1}{U} + \frac{1}{W}\right)} \quad (4)$$

Where $f_{\propto(1,\,d_e)}$ is the F Distribution Critical Values of F (α=5% significance level) (obtained from statistical tables) between 1 and d_e,(which is the degree of freedom of error) obtained from the analysis of variance, v_e is the variance (mean square) of error from the regression table. W is the number of effective replications = 3. U was calculated using Equation 5 [29]:

$$U = \frac{Total\ number\ of\ experiment}{1 + degree\ of\ freedom\ of\ control\ factors} \quad (5)$$

2.4.4 Regression Analysis (Modelling)

Linear regression analysis was conducted using Minitab software, generating an ANOVA table that included interaction effects to determine the significance of each processing parameter. This analysis was used to develop predictive mathematical models for all the responses as functions of the process parameters.

3. Results and Discussion

3.1 XRF for the Chemical Composition of Sand, Brass, Cast Iron and Aluminum Alloy

The XRF analysis results for the sand, brass, cast iron, and scrap engine top cylinder(aluminum) are presented in Tables 4 to Table 7, respectively. The elemental analysis revealed distinct dominant elements in each material used for casting and reinforcement; The aluminium alloy contains aluminium (76.61%), silicon (17.49%), and copper (1.90%), as shown in Table 4, typical of Al–Si alloys with improved strength and fatigue resistance due to copper. As shown in Table 5, the brown sand sample is predominantly silicon (89.51%), with phosphorus (7.41%) and potassium (1.70%), indicating a high silica content that provides good thermal stability. For the metallic chip reinforcements, as shown in Table 6, cast iron rich in iron (88.3%), carbon (3.7%), and silicon (2.8%) offers excellent thermal conductivity and heat retention, promoting faster and more uniform solidification of the molten aluminium. Similarly, Table 7 shows brass chips composed mainly of copper (64.00%), zinc (23.00%), and iron (3.20%), significantly enhance thermal transfer within the mold due to copper's superior conductivity. The inclusion of these metallic chips in the sand matrix improves the mold's heat extraction capability, leading to refined microstructures and improved mechanical properties in the final aluminium casting.

Table 4 *Elemental composition of the sample of aluminium alloy*

Element	Al	Si	Cu	Mg	Fe	Zn	Mn	S	Ca	Cr	Ni	Pb	Ti	Ba
%	76.61	17.49	1.9	1.28	1.14	0.85	0.20	0.15	0.09	0.07	0.07	0.06	0.03	0.02

Table 5 *Elemental composition of brown sand sample*

Element	Si	P	K	Fe	Al	Ca	Cl	Ti	Zr	Rb	Sr
%	89.51	7.41	1.70	0.70	0.43	0.11	0.07	0.05	0.02	0.01	0.01

Table 6 *Elemental composition of cast iron sample*

Element	Fe	C	Si	Al	Na	Ag	Ca	Cu	K
%	88.30	3.70	2.80	1.10	1.10	0.80	0.70	0.5	0.30

Table 7 *Elemental composition of brass sample*

Element	Cu	Zn	Fe	Ca	Pb	K	Ti	Sn	Mn
%	64.00	23.00	3.20	2.18	2.10	1.55	1.51	1.34	1.02

3.2 Fatigue Strength of Aluminum Alloy

Table 8 presents the results of the fatigue strength test conducted on the aluminum alloy samples and the control, along with their corresponding signal-to-noise (S/N) ratios. The experimental results reveal a clear enhancement in fatigue strength when aluminium alloy is cast using molding sand modified with metal chips, compared to the control sample produced with conventional molding sand. The highest fatigue strength was achieved in Run 16 (Chip Type 4, 40% chip content, 100 µm chip size), with a value of 71.00 MPa. This represents a 24.77% improvement over the control sample (56.90 MPa) cast in unmodified sand. The combination used in Run 16 likely provided optimal conditions for heat extraction and grain refinement during solidification, improving fatigue resistance. On the other hand, the lowest fatigue strength was recorded in Run 14 (Chip Type 4, 20% chip content, 300 µm chip size), at 57.11 MPa, which still shows a marginal improvement of 0.37% over the control. This suggests that introducing metal chips generally enhances fatigue performance at certain combinations, such as moderate chip content with larger particle sizes, which may offer limited benefits.

Table 8 *Fatigue strength results and their respective signal to noise ratios*

Runs	Factors			Fatigue Strength	
	Chips Type	Chips Content	Chips Size	Mean (MPa)	S/N ratio (dB)
1	1	10	100	70.08	36.91
2	1	20	200	59.82	35.54
3	1	30	300	57.69	35.22
4	1	40	400	63.79	36.10
5	2	10	200	65.30	36.30
6	2	20	100	64.00	36.12
7	2	30	400	66.50	36.46
8	2	40	300	64.50	36.19
9	3	10	300	61.00	35.71
10	3	20	400	64.50	36.19
11	3	30	100	63.50	36.06
12	3	40	200	67.52	36.59
13	4	10	400	58.00	35.27
14	4	20	300	57.11	35.13
15	4	30	200	61.60	35.79
16	4	40	100	71.00	37.03
Mean (T_m)				63.49	36.04
As-Cast Al (control)				56.90	

Overall, the results demonstrate that the effectiveness of chip reinforcement is significantly influenced by the chip content and particle size, with higher content and finer particles yielding better mechanical performance. The study confirms that modifying molding sand with suitable metal chip parameters can substantially improve the fatigue strength of aluminium alloy castings as a result of grain refinement. The results agree with the study conducted by Yang *et al.* [20], which showed an increase in fatigue strength of an aluminium alloy due to grain refinement.

3.3 Taguchi Optimization of Sand mold Factors for Fatigue Strength of Cast Aluminium Alloy

The higher-the-better objective function was used to observe the optimum and the most influential process parameters in the casting of aluminium alloy. This analysis gave signal-to-noise ratios, main effect plots for the mean of the fatigue strength and mean of signal-to-noise ratios, as presented in the discussions below:

3.3.1 Effect of Metal Chips Type, Metal Chips Content and Particle Size on Fatigue Strength

The effect of metal chip type, the weight percentage of the chips and the particle size of the chips in the sand mold on fatigue strength properties of the aluminium alloy is shown from Fig. 4 to Fig. 6. Fig. 4 shows the influence of different metal chip types used in sand molds on the fatigue strength of aluminium alloy castings. The results reveal that Chip Type 2 yielded the highest fatigue strength, reaching approximately 65.08 MPa. This improvement can be attributed to the combined chips enhanced thermal conductivity and heterogeneous nucleation effects, which promote rapid heat extraction and finer grain structures during solidification. The synergy between brass and cast iron likely creates a balanced thermal gradient and structural framework within the mold, leading to improved fatigue resistance. In contrast, Chip Type 4 (brass chips only) resulted in the lowest fatigue strength, around 61.9 MPa, possibly due to insufficient cooling rate and lack of structural support compared to hybrid mixtures. These findings align with Anil Kumar et al. [36], who observed that incorporating thermally conductive reinforcements like garnet in sand molds improved mechanical performance through grain refinement caused by cryogenic effects. Figure 4 shows an optimum fatigue strength of 65.08 MPa when using cast iron chips as chills in a sand mold.

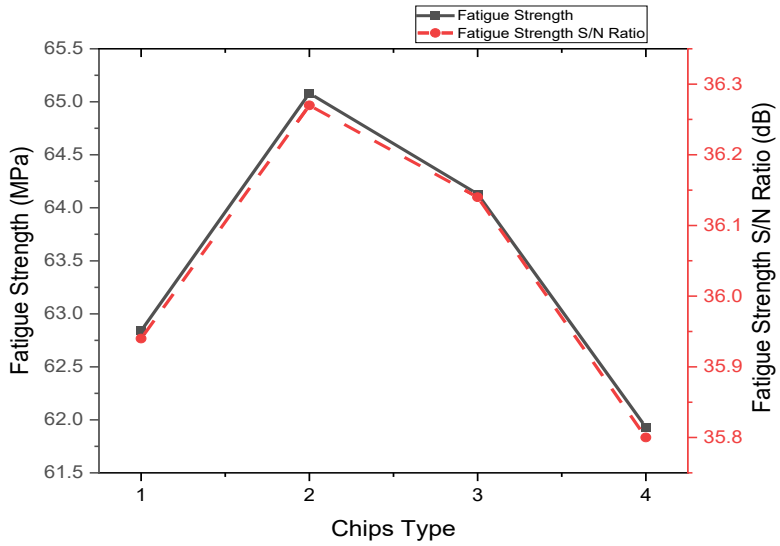

Fig. 4 *Variation of fatigue strength with metal chip type*

Fig. 5 shows the influence of chip content (wt%) in the sand mold on the fatigue strength and signal-to-noise (S/N) ratio of aluminium alloy castings. The highest fatigue strength (66.7 MPa) was achieved at a 40 wt% concentration, while the lowest value was observed at a 20 wt% concentration. This pattern indicates a non-linear response, where the initial reduction in fatigue strength up to 20% may be attributed to inadequate bonding or chip agglomeration, which can disturb the mold's integrity and promote heterogeneous solidification.

At higher chip contents, however, both the fatigue strength and S/N ratio increased markedly. This improvement is likely due to the enhanced thermal conductivity introduced by the metallic chips, which promotes

more uniform heat extraction and, consequently, finer grain structures. The resulting grain refinement contributes significantly to improved fatigue resistance, as finer grains reduce the likelihood of crack initiation and slow down crack propagation under cyclic loading. Therefore, the optimum fatigue strength of 66.7 MPa at 40 wt% correlates strongly with the refined microstructure observed at this chip concentration.

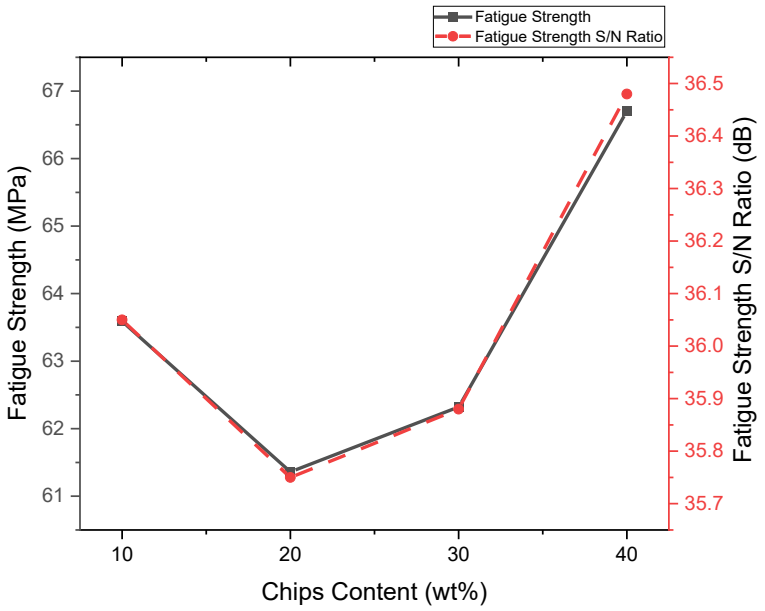

Fig. 5 *Variation of fatigue strength with chip addition*

Fig. 6 shows that an increase in chip particle size decreases the material's fatigue strength, but the alloy's fatigue strength increases with a further increase. The decrease may be attributed to the reduced efficiency of heat extraction associated with larger particles. Smaller particles possess a higher surface-area-to-volume ratio, which enhances thermal conductivity within the mold and promotes rapid, uniform heat dissipation during solidification. The trend of this result agrees with related studies by Nandagopal et al. [37]. The analysis showed an optimum fatigue strength of 67.14 MPa at a chip particle size of 100 µm.

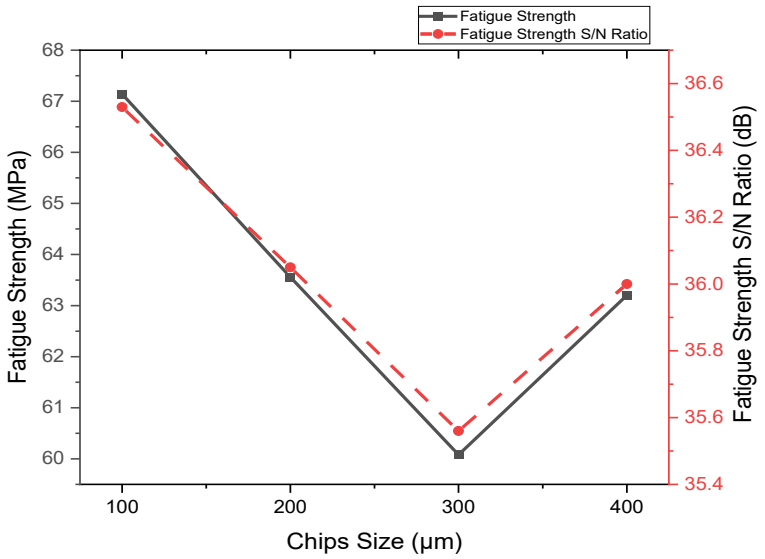

Fig. 6 *Variation of fatigue strength with chip particle size*

3.3.2 Optimum Combination for Fatigue Strength of the Aluminum Alloy

From the Fig. 4 to Fig. 6, the optimum levels of factors for the sand mould that give the best fatigue strength values are; brass/cast iron metal chips (A) (level 2), metal chips content (B) at 40 %wt (level 4), and chips particles size (C) of 100 µm (level 1). Therefore, the predicted optimum combination is denoted by $A_2 - B_4 - C_1$ for fatigue strength.

3.3.3 Estimating the Optimal Fatigue Strength

From the analysis so far, using the optimal settings of the moulding sand process ($A_2 - B_4 - C_1$), an optimal fatigue strength of 79.93 MPa for the aluminium alloy was obtained by using Equation 2.

3.3.4 Confirmation Test

The result of the fatigue strength (FS) confirmation test is shown in Table 9. From the table, an average fatigue strength of 73.41 MPa was obtained.

Table 9 *Fatigue strength test confirmation result*

Runs	Factors			FS (MPa)
(S/N)	A	B (wt%)	C (µm)	Average
1	2	40	100	73.41

The result of the predicted and the experimental fatigue strength values of the optimal processing parameters ($A_2 - B_4 - C_1$), of the hybrid aluminium alloy, are shown in Table 10, where the error percentage was also calculated.

Table 10 *Confirmatory results comparison at the optimal level*

	Optimal process parameter settings	Predicting value	Experimental value	% Error
S/N ratio (dB)	A2 – B4 – C1	37.20	37.31	0.29
Fatigue Strength (MPa)		71.93	73.41	2.02

3.4 Regression Analysis (Modelling)

Table 11 shows the ANOVA results obtained for the fatigue strength of the aluminium alloy. From the table, at the significant level of 0.05, the regression model, all the factors, and all the interactions were found significant to the fatigue strength since their p-value is less than 0.05.

Table 11 *Analysis of variance of fatigue strength for the aluminium alloy*

Source	DF	Adj SS	Adj MS	F-Value	P-Value	% Contribution
Regression	8	257.90	32.24	364.16	0.000	
Chip Type (A)	1	0.75	0.75	8.45	0.023	0.24
Chips Content (B)	1	88.67	88.67	1001.66	0.000	28.37
Chip Size (C)	1	35.53	35.53	401.34	0.000	11.37
A2	1	19.65	19.65	221.94	0.000	6.29
B2	1	43.79	43.79	494.68	0.000	14.01
C2	1	44.99	44.99	508.22	0.000	14.39
A*B	1	73.27	73.27	827.71	0.000	23.44
A*C	1	5.31	5.31	60.00	0.000	1.70
Error	7	0.62	0.09			0.20
Total	15	312.58				100

The predictive mathematical model for the fatigue strength (FS) is presented in Equation 6.

$$FS = 91.444 - 1.344\,A - 1.6399\,B - 0.09262\,C - 1.1081\,A^2 + 0.016544\,B^2 + 0.000168\,C^2 + 0.2886A * B + 0.000777\,A * C \quad (6)$$

The developed regression model for fatigue strength demonstrates an excellent fit, with R-square, adjusted R-square, and predicted R-square values of 99.76%, 99.49%, and 98.50%, respectively. These high values indicate a strong correlation between fatigue strength and the factors considered in sand mould preparation. According to Ibrahim et al. [27], Dan-Asabe et al. [38] and Siviah and Chakradh [28], an R-square value above 75% is considered satisfactory. Moreover, the model is reliable for predicting values within and beyond the experimental range, as the difference between the adjusted and predicted R-squared values is less than 20% [38-39, 40]. Fig. 7 illustrates the close agreement between the predicted and experimental fatigue strength values across 16 runs.

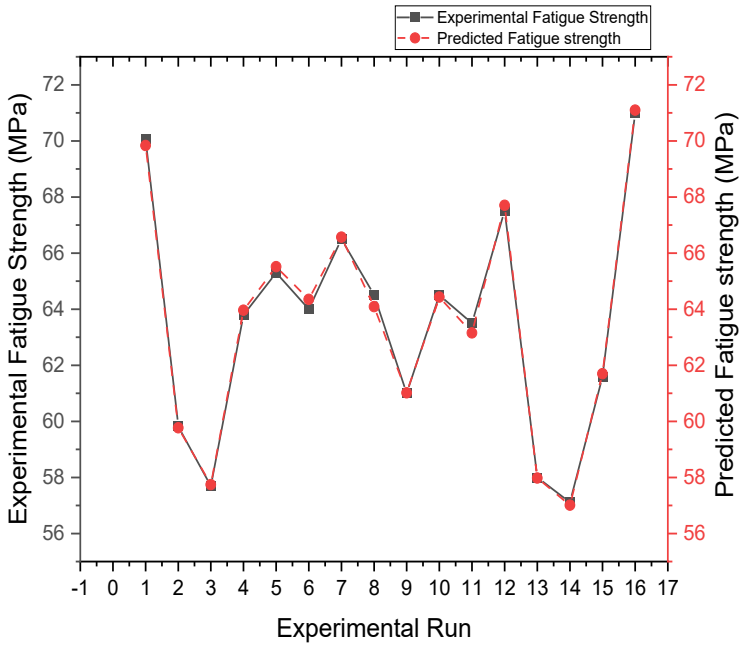

Fig. 7 *Experimental and simulated (modelled) fatigue strength (FS)*

3.4.1 Confidence Interval (CI)

A confidence interval of ±1.34 was evaluated using Equation 3. The fatigue strength obtained from the confirmatory test was 73.41 MPa, which falls within the calculated confidence interval range for fatigue strength ($72.07 < FS_{experimental} < 74.75$). This result confirms the acceptability of the optimum fatigue strength value prediction within the confidence interval of 95%.

3.5 Optimal Properties of the Molding Sand and Cast Aluminum

Fig. 8 shows the results for compactibility (COM), green compressive strength (GCS), and dry compressive strength (DCS) of the foundry sand used in producing the optimal aluminium alloy for fatigue strength testing. The sand used for the control casting (without metal chips) recorded GCS, DCS, and COM values of 57.75 kN/m^2, 220 kN/m^2, and 44%, respectively. In contrast, the sand mixed with brass and cast iron chips in a 1:2 ratio used for fatigue-strength test samples achieved higher values: 69.5 kN/m^2 (GCS), 270 kN/m^2 (DCS), and 46% (COM). These values fall within the acceptable ranges for aluminum alloy casting, as Sahoo et al. [41]and Guma [42] recommended.

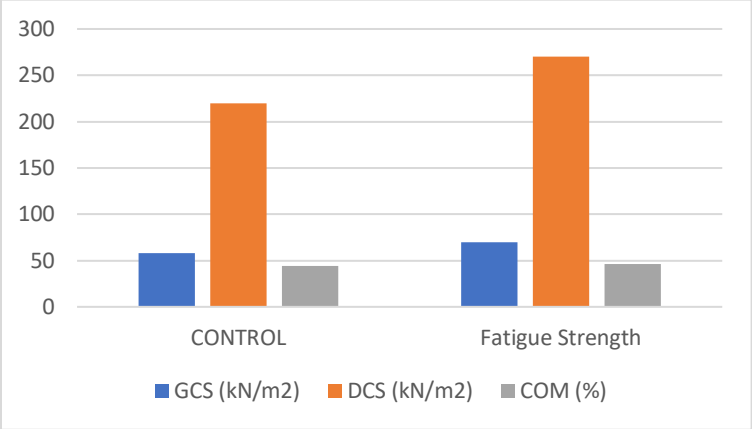

Fig. 8 *Bar chart with standard deviation of green, dry compression strength and compactibility optimal combination for molding sand for fatigue sample*

3.6 Fatigue and SEM of the Optimal and Control Cast Aluminum Alloy

Fig. 9(a) and (b) display the SEM micrographs of the optimized and control specimens, respectively. In the images, the aluminum alloy matrix appears in grey. At the same time, the bright dendritic regions and darker areas correspond to Si-eutectoid phases, as described by Mourad et al. [43] and Ibrahim and Yawas [39]. Notably, the optimized sample exhibits a much finer microstructure than the control, which likely contributed to its superior fatigue strength of 73.41 MPa compared to 56.90 MPa recorded for the control.

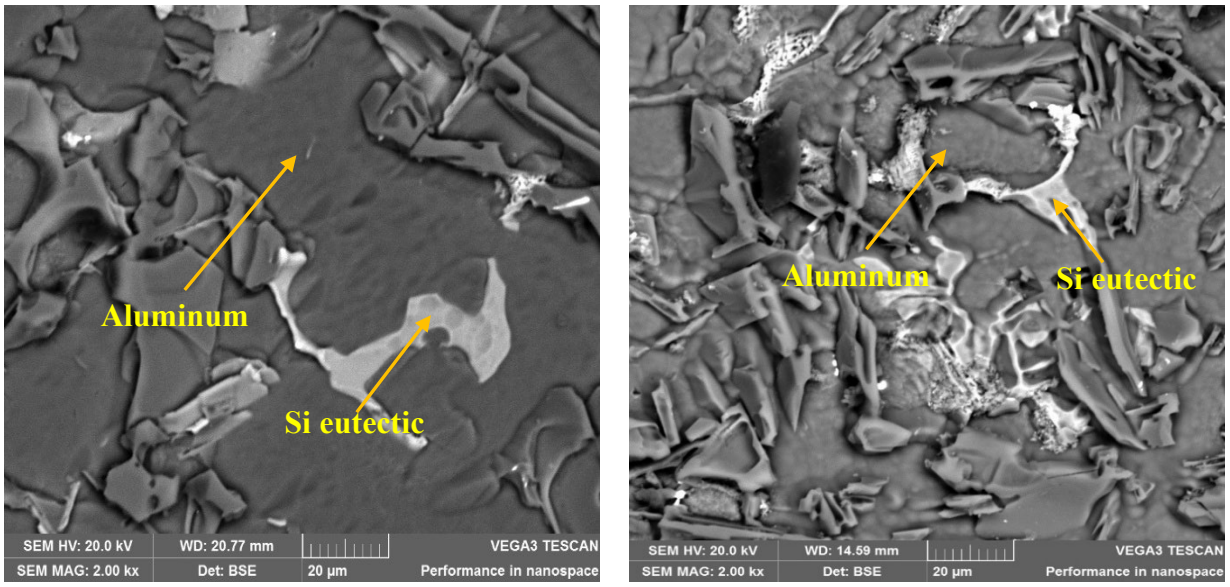

(a) **(b)**

Fig. 9 *SEM images; (a) Optimal sample; (b) Control sample*

3.7 Thermal Analysis of the Optimal Cast Aluminum Alloy

The thermo-gravimetric and differential thermo-gravimetric analyses (TGA/DTA) curves in Fig. 10 demonstrate a two-step weight loss for optimal cast aluminum alloy upon heating between 30 °C and 1000 °C under a nitrogen gas environment.

The thermal behavior of both the control and optimized aluminum castings was evaluated using thermogravimetric and differential thermal analysis (TGA/DTA), and the results are presented in Figure 10. The initial weight loss observed for the control sample was 1.78%, while the optimized sample recorded a slightly higher loss of 1.99%, both attributed to the evaporation of surface-adsorbed moisture.

The major decomposition phase for the optimized composite occurred between 359.32 °C and 569.59 °C, with a total mass loss of 80.78%. Conversely, the control sample experienced significant decomposition earlier, within the range of 269.94 °C to 524.24 °C, and exhibited a higher mass loss of 83.29%. This translates to a 3.01%

reduction in thermal degradation for the optimized casting, indicating enhanced thermal stability resulting from metal chips in the molding sand.

Moreover, the onset temperature for decomposition was markedly higher in the optimized sample (359.32 °C) compared to the control (269.94 °C), signifying a 33.11% improvement in thermal resistance. This increase indicates the improved heat resistance conferred by better heat extraction in the composite molding sand and the lower oxidation susceptibility of the constituents. The enhanced thermal stability is also linked to reduced volatilization of alloying elements and more stable intermetallic phase transformations in the optimized structure.

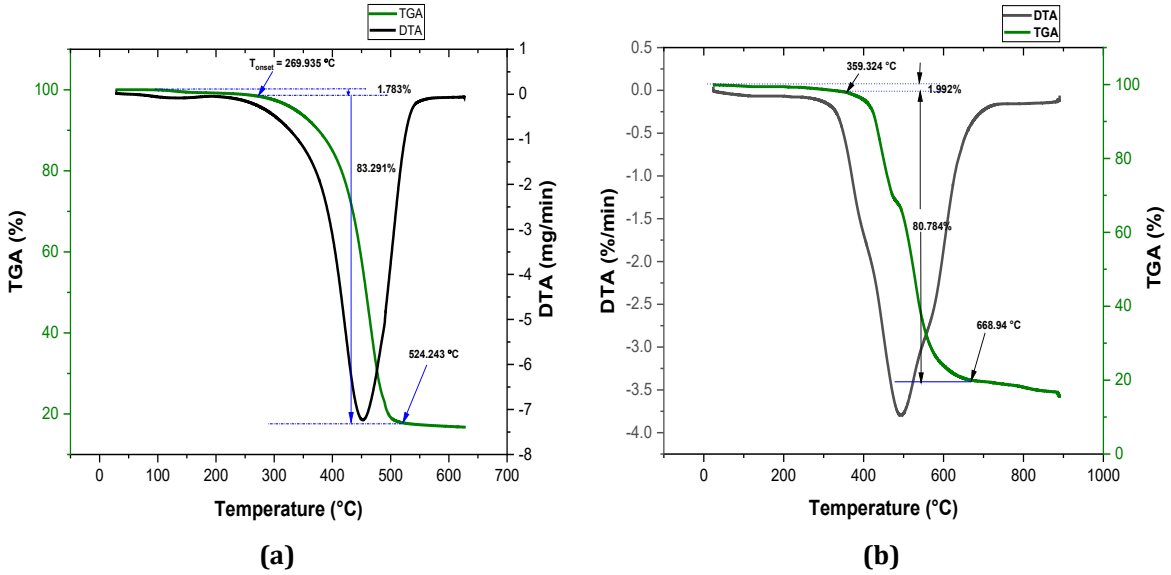

Fig. 10 *TGA-DTA curves showing thermal decompositions of the control and optimal cast aluminum alloy*

4. Conclusion

This study focuses on the eco-friendly optimization of fatigue strength in sand-cast aluminium alloys using waste metal chips as mould additives through the Taguchi design of experiments. Scrap aluminium alloy (from engine blocks), brown sand, cast iron chips, and brass chips were successfully utilized, and the resulting castings were developed and characterized. Based on the findings, the following conclusions are drawn:

i. The XRF showed the presence of aluminium (76.61%), silicon (17.49%), and magnesium (1.28%) as the major elements in the aluminium alloy and silicon (89.51%). These elements shows that the scrap aluminum engine block is of Alxxxx series. The major constituents of brown sand are phosphorus (7.41%), and potassium (1.7%). In cast iron, iron (88.3%), carbon (3.7%), and silicon (2.3%). Meanwhile, in brass, the major elements were copper (64%), zinc (23%), and iron (3.2%). Identifying these chemical compositions is therefore vital, as they determine the thermal behaviour of the mould/metal system, influence grain refinement, and ultimately govern the microstructure and fatigue resistance of the cast aluminium alloy.

ii. When compared with the as-cast aluminium alloy, the fatigue test results of the produced aluminium alloys show a 24.78% increase in fatigue strength, respectively.

iii. The optimal combination of the factors (chip types, chips weight per cent and chips particles sizes) for the production of the aluminium alloy using the Taguchi analysis was brass/cast iron metal chips (level 2), chips content of 40 %wt (level 4), and chips particles size of 100 µm (level 1). The Taguchi optimization shows an improvement in the cast aluminium alloy properties by an increase of 28.30 % in the fatigue strength values, compared with the as-cast aluminium alloy. The scanning electron microscopy observation of the optimal sample revealed fine-grain refinement compared with the control. The optimized aluminum casting exhibited a 3.01% reduction in mass loss and a 33.11% increase in decomposition onset temperature compared to the control, indicating improved thermal stability.

iv. The foundry sand with metal chips improved green compressive strength by 20.33%, dry compressive strength by 22.73%, and compactibility by 4.55% compared to the control.

Acknowledgement

The authors would like to thanks Prof. D. S. Yawas, Prof. T. Ause, and Prof. M. O. Afolayan, for their steadfast support, expert guidance, and invaluable encouragement throughout the course of this research.

Conflict of Interest

Authors declare that there is no conflict of interests regarding the publication of the paper.

Author Contribution

The authors confirm contribution to the paper as follows: ***study conception and design****: Maaruf Isyaku, Danjuma Saleh Yawas, Mathew Olatunde Afolayan, Terva Ause;* ***data collection****: Maaruf Isyaku;* ***analysis and interpretation of results****: Maaruf Isyaku, Tanimu Kogi Ibrahim;* ***draft manuscript preparation****: Maaruf Isyaku, Tanimu Kogi Ibrahim. All authors reviewed the results and approved the final version of the manuscript.*

References

[1] Aliemeke, B., Ehibor, O. & Aideloje, V. (2018) The effect of sand casting process parameters on the fatigue strength of aluminium–silicon alloy using Taguchi design and genetic algorithm, *Journal of Chemical, Mechanical and Engineering Practices*, 7(1–3), 39–49.

[2] Xu, W., de Boer, O., Grasso, M., Harrison, M. F., Carless, O. & StLeger-Harris, C. (2023) On a numerical methodology to assess the fatigue life of connecting rods, *Proceedings of the Institution of Mechanical Engineers, Part D: Journal of Automobile Engineering*, 238(10–11), 3232–3241. https://doi.org/10.1177/09544070231180996

[3] Sharma, A., Oh, M. C. & Ahn, B. (2020) Recent advances in very high cycle fatigue behavior of metals and alloys—A review, *Metals*, 10(9), 1200. https://doi.org/10.3390/met10091200

[4] Chetan, J. S., Khushbu, P. C. & Fajalhusen, P. (2012) A review of the fatigue analysis of automobile frames, *International Journal of Advanced Computer Research*, 2(4), 103.

[5] Antaki, G. & Gilada, R. (2015) Design basis loads and qualification, *Nuclear Power Plant Safety and Mechanical Integrity*, 27–102. https://doi.org/10.1016/b978-0-12-417248-7.00002-3

[6] Samuel, E., Samuel, A. M., Songmene, V. & Samuel, F. H. (2023) A review on the analysis of thermal and thermodynamic aspects of grain refinement of aluminum–silicon-based alloys, *Materials*, 16(16), 5639.

[7] Wang, G., Che, X., Zhang, Z., Zhang, H., Zhang, S., Li, Z. & Sun, J. (2020) Microstructure and low-cycle fatigue behavior of Al-9Si-4Cu-0.4Mg-0.3Sc alloy with different casting states, *Materials*, 13(3), 638. https://doi.org/10.3390/ma13030638

[8] Alzubi, F., Timko, M., Li, Y. J., Toal, R., Tovalin, K. & Es-Said, O. (2019) Large versus small grain sizes on fatigue life of aluminum aircraft wheels, *Defect and Diffusion Forum*, 391, 174–194. https://doi.org/10.4028/www.scientific.net/ddf.391.174

[9] Shou, W., Yi, D., Liu, H., Tang, C., Shen, F. & Wang, B. (2016) Effect of grain size on the fatigue crack growth behavior of 2524-T3 aluminum alloy, *Archives of Civil and Mechanical Engineering*, 16(3), 304–312. https://doi.org/10.1016/j.acme.2016.01.004

[10] Mu, P., Nadot, Y., Nadot-Martin, C., Chabod, A., Serrano-Munoz, I. & Verdu, C. (2014) Influence of casting defects on the fatigue behavior of cast aluminum AS7G06-T6, *International Journal of Fatigue*, 63, 97–109. https://doi.org/10.1016/j.ijfatigue.2014.01.011

[11] Hafeez, F., Ahmed, N., Ali, M. A., Farooq, M. U., AlFaify, A. Y. & Rehman, A. U. (2022) A comprehensive efficiency evaluation of conventional and ablation sand casting on the example of the AlSi7Mg alloy impeller, *International Journal of Advanced Manufacturing Technology*, 121(5–6), 3653–3672. https://doi.org/10.1007/s00170-022-09538-w

[12] Guan, R.-G. & Tie, D. (2017) A review on grain refinement of aluminum alloys: Progresses, challenges and prospects, *Acta Metallurgica Sinica (English Letters)*, 30(5), 409–432. https://doi.org/10.1007/s40195-017-0565-8

[13] Hurtalová, L., Tillová, E., Chalupová, M., Belan, J. & Uhríčik, M. (2016) The influence of two different casting moulds on the fatigue properties of the Al–Si–Cu cast alloy, *Advanced Structured Materials*, 61–70. https://doi.org/10.1007/978-981-10-1082-8_6

[14] United Nations (2015) Sustainable Development Goal 13: Take urgent action to combat climate change and its impacts, *United Nations*. https://sdgs.un.org/goals/goal13

[15] Zych, J., Mocek, J., Snopkiewicz, T. & Jamrozowicz, Ł. (2015) Thermal conductivity of moulding sand with chemical binders: Attempts of its increasing, *Archives of Metallurgy and Materials*, 60(1), 351–357. https://doi.org/10.1515/amm-2015-0058

[16] Małek, M., Kadela, M., Terpiłowski, M., Szewczyk, T., Łasica, W. & Muzolf, P. (2021) Effect of metal lathe waste addition on the mechanical and thermal properties of concrete, *Materials*, 14(11), 2760. https://doi.org/10.3390/ma14112760

[17] Koroyasu, S. (2025) Effect of sand material type on heat absorbing properties of mold in expendable pattern casting process of aluminum alloy castings, *Materials Transactions*, 66(4), 426–433. https://doi.org/10.2320/matertrans.f-m2024815

[18] Olanipekun, K. A. (2020) Assessment of factors influencing the development and sustainability of small-scale foundry enterprises in Nigeria: A case study of Lagos State, *Asian Journal of Social Sciences and Management Studies*, 7(4), 288–294

[19] Sadarang, J., Nayak, R. K. & Panigrahi, I. (2022) Evaluation of compactibility and shear strength of sand-less casting mould for sand casting process, *Lecture Notes in Mechanical Engineering*, 449–457. https://doi.org/10.1007/978-981-16-8341-1_37

[20] Yang, B.-C., Chen, S.-F., Song, H.-W., Zhang, S.-H., Chang, H.-P., Xu, S.-W., Zhu, Z.-H. & Li, C.-H. (2022) Effects of microstructure coarsening and casting pores on the tensile and fatigue properties of cast A356-T6 aluminum alloy, *Materials Science and Engineering A*, 857, 144106. https://doi.org/10.1016/j.msea.2022.144106

[21] Chen, H., Liu, S., Wang, P., Wang, X., Liu, Z. & Aldakheel, F. (2024) Effect of grain structure on fatigue crack propagation behavior of 2024 aluminum alloy under different stress ratios, *Materials & Design*, 244, 113117. https://doi.org/10.1016/j.matdes.2024.113117

[22] Elanchezhian, C. & Vijaya, M. (2016) *Production Technology (Manufacturing Processes)*, Laxmi Publications Pvt Ltd, New Delhi.

[23] Kang, J.-w., Shangguan, H.-l., Peng, F., Xu, J.-y., Deng, C.-y., Hu, Y.-y., Yi, J.-h., Huang, T., Zhang, L.-j. & Mao, W.-m. (2021) Cooling control for castings by adopting skeletal sand mold design, *China Foundry*, 18(1), 18–28. https://doi.org/10.1007/s41230-021-0150-7

[24] Ibrahim, T., Yawas, D. S. & Aku, S. Y. (2013a) Effects of gas metal arc welding techniques on the mechanical properties of duplex stainless steel, *Journal of Minerals and Materials Characterization and Engineering*, 1, 222–230.

[25] Ibrahim, T., Leva, I., Iliyasu, I. & Yawas, D. (2016) Comparative analysis of neem and lubricating (85W90) oils as quenchants on the mechanical properties of shield metal arc welded duplex stainless steel, *International Journal of Scientific and Engineering Research*, 7(4), 1825–1836.

[26] Ibrahim, T., Yawas, D. S. & Aku, S. Y. (2013b) Effects of shield metal arc welding techniques on the mechanical properties of duplex stainless steel, *Advances in Applied Research*, 4(5), 190–201.

[27] Ibrahim, T. K., Yawas, D. S., Thaddaeus, J., Danasabe, B., Iliyasu, I., Adebisi, A. A. & Ahmadu, T. O. (2024a) Development, modelling and optimization of process parameters on the tensile strength of aluminum reinforced with pumice and carbonated coal hybrid composites for brake disc application, *Scientific Reports*, 14(1), 16999.

[28] Sivaiah, P. & Chakradhar, D. (2019) Modeling and optimization of sustainable manufacturing process in machining of 17-4 PH stainless steel, *Measurement*, 134, 142–152.

[29] Alabi, A. A., Samuel, B. O., Peter, M. E. & Tahir, S. M. (2022) Optimization and modelling of the fracture inhibition potential of heat-treated doum palm nut fibres in phenolic resin matrix composites: A Taguchi approach, *Functional Composites and Structures*, 4(1), 015004. https://doi.org/10.1088/2631-6331/ac5466

[30] Ibrahim, T. K., Yawas, D. S., Dan-asabe, B. & Adebisi, A. A. (2023a) Manufacturing and optimization of the effect of casting process parameters on the compressive strength of aluminum/pumice/carbonated coal hybrid composites: Taguchi and regression analysis approach, *International Journal of Advanced Manufacturing Technology*, 1–1. https://doi.org/10.1007/s00170-023-10923-2

[31] Ibrahim, T. K., Iliyasu, I. & Abiodun, P. C. (2024b) Application of Taguchi methods and regression analysis to optimize process parameters and reinforcements for maximizing composite coefficient of friction for brake disc application, *Journal of Sustainable Materials Processing and Management*, 4(1), 89–105.

[32] Ibrahim, T. K., Yawas, D. S., Dan-asabe, B. & Adebisi, A. A. (2023b) Taguchi optimization and modelling of stir casting process parameters on the percentage elongation of aluminium, pumice and carbonated coal composite, *Scientific Reports*, 13, 2915. https://doi.org/10.1038/s41598-023-29839-8

[33] Ibrahim, T. K., Yawas, D. S., Danasabe, B. & Adebisi, A. A. (2023c) Optimization and statistical modeling of the thermal conductivity of a pumice powder and carbonated coal hybrid reinforced aluminum metal matrix composite for brake disc application: A Taguchi approach, *Functional Composites and Structures*, 5(1), 015008. https://doi.org/10.1088/2631-6331/acc0d1

[34] Samuel, B. O., Alabi, A. A., Lawal, S. A., Peter, E. & Ibrahim, T. K. (2024) Optimizing the effect of heat treatment on the mechanical properties of Hyphaene thebaica nut: A machine learning and Taguchi approach, *Heliyon*, 10(19), e38899. https://doi.org/10.1016/j.heliyon.2024.e38899

[35] Ibrahim, T. K., Thaddaeus, J., Popoola, C. A., Iliyasu, I. & Alabi, A. A. (2024c) Improvement of wear rate properties of a brown pumice and coal ash particulates reinforced aluminum composite for brake manufacturing through optimization and modelling, *Jordan Journal of Mechanical and Industrial Engineering*, 18(4).

[36] Anil Kumar, B. K., Ananthaprasad, M. G. & GopalaKrishna, K. (2016) Action of cryogenic chill on mechanical properties of nickel alloy metal matrix composites, *IOP Conference Series: Materials Science and Engineering*, 149, 012116. https://doi.org/10.1088/1757-899X/149/1/012116

[37] Nandagopal, M., Sivakumar, K., Sengottuvelan, M. & Velmurugan, S. (2021) Optimization of process parameters to reduce green sand casting defects, *Springer Proceedings in Materials*, 655–661. https://doi.org/10.1007/978-981-15-8319-3_65

[38] Dan-Asabe, B., Yaro, S., Yawas, D. & Aku, S. (2019) Statistical modeling and optimization of the flexural strength, water absorption and density of a doum palm–Kankara clay filler hybrid composite, *Journal of King Saud University–Engineering Sciences*, 31(4), 385–394.

[39] Ibrahim, T. K. & Yawas, D. S. (2025) Multifaceted analysis of aluminum–coal ash–pumice composites for enhanced brake disc specific heat capacity, *Jurnal Mekanikal*, 22–40. https://doi.org/10.11113/jm.v48.509

[40] Rai, A., Mohanty, B. & Bhargava, R. (2016) Supercritical extraction of sunflower oil: A central composite design for extraction variables, *Food Chemistry*, 192, 647–659.

[41] Sahoo, P. K., Pattnaik, S. & Sutar, M. K. (2020) Investigation of the foundry properties of the locally available sands for metal casting, *Silicon*, 13(11), 3765–3775. https://doi.org/10.1007/s12633-020-00677-x

[42] Guma, T. N. (2012) Characteristic foundry properties of Kaduna river sand, *International Journal of Engineering and Science*, 1(11), 3–8.

[43] Mourad, A.-H. I., Christy, J. V., Krishnan, P. K. & Mozumder, M. S. (2023) Production of novel recycled hybrid metal matrix composites using optimized stir squeeze casting technique, *Journal of Manufacturing Processes*, 88, 45–58. https://doi.org/10.1016/j.jmapro.2023.01.040

[44] Yawas, D. S., Aku, S. Y. & Aluko, S. O. (2014) Fatigue behavior of welded austenitic stainless steel in different environments, *Results in Physics*, 4, 127–134. https://doi.org/10.1016/j.rinp.2014.03.005